

Coordination Chemistry of Cyclic Disilylated Germynes and Stannylenes with Group 11 Metals

Johann Hlina,[†] Henning Arp,[†] Małgorzata Walewska,[†] Ulrich Flörke,[‡] Klaus Zangger,[§] Christoph Marschner,^{*,†} and Judith Baumgartner^{*,§}

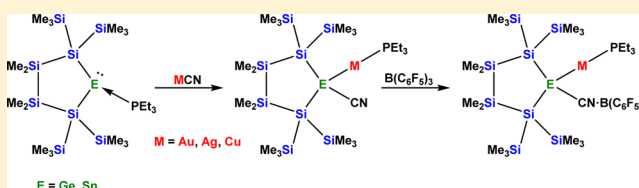
[†]Institut für Anorganische Chemie, Technische Universität Graz, Stremayrgasse 9, 8010 Graz, Austria

[§]Institut für Chemie, Karl Franzens Universität Graz, Stremayrgasse 9 and Heinrichstraße 28, 8010 Graz, Austria

[‡]Zentrale Analytik, Department Chemie, Universität Paderborn, Warburger Straße 100, 33098 Paderborn, Federal Republic of Germany

Supporting Information

ABSTRACT: Reactions of Et₃P adducts of bisilylated germynes and stannylenes with gold, silver, and copper cyanides led to cyanogermyl or -stannyl complexes of the respective metals. In the course of the reaction the phosphine moved to the metal, while the cyanide migrated to the low-coordinate group 14 element. The respective gold complexes were found to be monomeric, whereas the silver and copper complexes exhibited a tendency to dimerize in the solid state. Attempts to abstract the phosphine ligand with B(C₆F₅)₃ led only to the formation of adducts with the borane coordinating to the cyanide nitrogen atom.



1. INTRODUCTION

The organometallic chemistry of the group 10 metals Ni, Pd, and Pt has been in the focus of chemists now for decades, but related research on group 11 metals Ag and Au has been neglected for a long time. Of the group 11 metals only copper chemistry was studied with much interest, because its value as a synthetically useful metal had been established early, in particular for a number of coupling reactions such as the Ullmann,¹ Glaser–Hay,² and Cadot–Chodkiewicz³ reactions. The last some 20 years have brought a paradigm shift, and silver and in particular gold have become very valuable metals for a number of catalytic processes,^{4,5} exhibiting properties that complement chemistry developed earlier for palladium and nickel.

Compared to classical organometallic compounds with carbon–metal bonds, related substances where carbon is replaced by its heavier congeners silicon, germanium, tin, and lead have also received much less attention. In 1962 Glockling and Hooten synthesized the first germanium–group 11 compounds by metathesis reactions of triphenylgermyl lithium and the corresponding group 11 chloride(I) phosphine complexes.⁶ The first group 11 stannyl complexes were obtained soon after by reaction of group 11 metal chloride(I) triphenylphosphine complexes with SnCl₂.⁷ While the reaction of metal halides with anionic main-group compounds is rather straightforward, the second reaction is more interesting, as it can be considered as the insertion of a stannylene into a metal–halide bond. This synthetic strategy has proven rather useful and turned out to be surprisingly general.^{8,9} An interesting conceptual consequence of such reactivity is the fact that the formed ligand can be regarded either as a stannyl group or

alternatively as a base-stabilized stannylene ligand with chloride acting as base. Examples of gold complexes where both types of these ligands (base-stabilized and nonstabilized germynes) coordinate to one gold atom were reported only recently.¹⁰ Earlier studies by Klinkhammer and co-workers showed that reaction of a bis[tris(trimethylsilyl)silyl]stannylene with an arylcopper species led to the formation of a copper stannylene complex, where the aryl group on copper was exchanged with one of the tris(trimethylsilyl)silyl groups.¹¹ Tolman and co-workers later showed that coordination of Lappert's diamino-germylene [(Me₃Si)₂N]₂Ge to a β-diketimate complex of Cu(I) gave a non-base-stabilized germylene copper complex.¹² The interaction between carbenes, silylenes, or germynes and group 11 chlorides has also been studied theoretically.¹³ Anandhi and Sharp reported solution emission spectra (excitation wavelength: 385 nm) of their diamidochlorogermyl gold phosphine complexes in toluene to show bands between 540 and 600 depending on the type of phosphine.^{9,14}

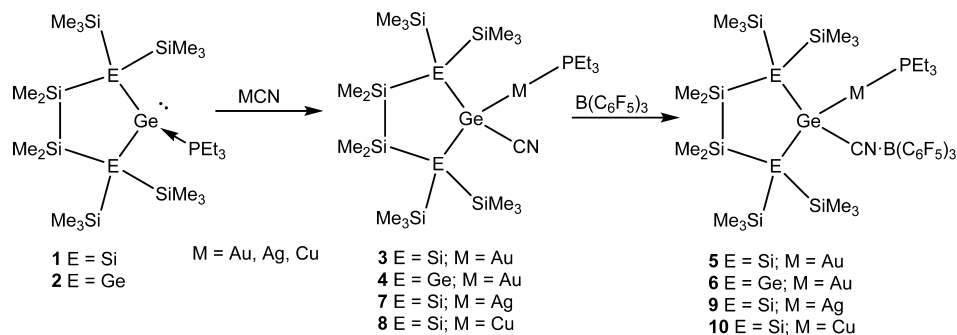
2. RESULTS AND DISCUSSION

In the course of studies on the coordination chemistry of disilylated stannylenes and germynes we recently found that the reaction of stabilized examples of these compounds with group 10 d¹⁰ metals complexes led to the isolation of silastannene and silagermene complexes of platinum and palladium.^{15–17} The formation of the initially expected stannylene and germylene complexes was possible only in the case of nickel.¹⁵ In order to study the coordination chemistry of

Received: June 27, 2014

Published: November 26, 2014

Scheme 1. Reactions of Germylene Phosphine Adducts with Group 11 Cyanides



Scheme 2. Formation of Gold Stannylene Complexes 12 and 13

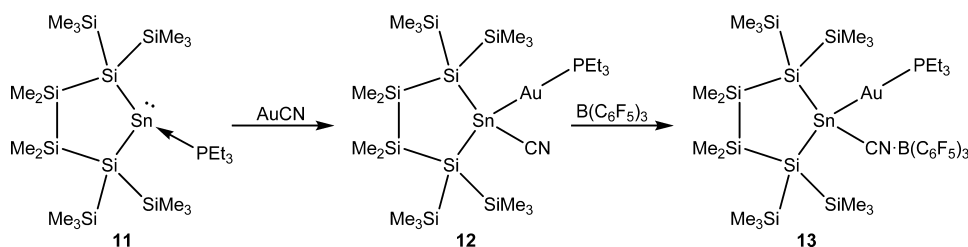


Table 1. NMR Spectroscopic Data

compound	Si _q	SiMe ₃	SiMe ₂	³¹ P	¹¹⁹ Sn	¹¹ B	¹⁹ F
1	-127.1 (15 Hz)	-7.9 (br)	-22.7 (10 Hz)	14.8	n.a.	n.a.	n.a.
2	n.a.	-2.0 (14 Hz)/ -4.1 (8 Hz)	-16.9 (8 Hz)	15.0	n.a.	n.a.	n.a.
3	-110.4 (7 Hz)	-5.6/-8.4	-21.4 (5 Hz)	49.0	n.a.	n.a.	n.a.
4	n.a.	0.2/-3.7	-15.3 (5 Hz)	48.8	n.a.	n.a.	n.a.
5	-110.0 (6 Hz)	-5.5/-7.9	-23.2 (3 Hz)	47.5	n.a.	-11.5	-132.3/-158.0/-164.3
6	n.a.	0.8 (3 Hz)/-2.6	-16.3 (3 Hz)	47.6	n.a.	-11.9	-132.3/-158.2/-164.4
7	-114.2	-5.8/-9.0	-21.4	4.7	n.a.	n.a.	n.a.
8	-115.6	-6.6/-8.8	-22.1	-16.5	n.a.	n.a.	n.a.
9	-114.6 (dd, 11 Hz, 4 Hz)	-5.9 (3 Hz)/ -8.4 (2 Hz)	-22.7 (dd, 3 Hz, 2 Hz)	7.4 (433/366 Hz)	n.a.	11.7	132.7/-158.2/-164.4
10	-115.3 (4 Hz)	-6.0/-8.6	-22.6	-7.6	n.a.	-11.7	-132.8/-158.1/-164.3
11	-137.9 (16 Hz)	-4.2/-7.4	-20.0	-1.0	-224.4 (2220 Hz)	n.a.	n.a.
12	-125.8	-4.4/-7.4	-19.1	49.5	-126.0 (1633 Hz)	n.a.	n.a.
13	-122.7 (9 Hz)	-3.9/-7.1	-20.0 (4 Hz)	50.1	31.1 (1545 Hz)	-11.2	-132.6/-158.1/-164.4

these stannylenes¹⁸ and germylenes¹⁹ with other d¹⁰ complexes, we decided to turn to group 11 M(I) complexes.

Synthesis. Reactions of PEt₃-stabilized germylenes **1** and **2** with gold cyanide in benzene gave the respective complexes **3** and **4** (Scheme 1). In contrast to related reactions with group 4 metallocenes^{20,21} and nickel,¹⁵ which led to base-free tetrylene metal complexes, the reaction with gold cyanide was found to involve the transfer of a metal ligand, cyanide, to the germylene. The latter can thus be regarded either as a base-stabilized germylene or alternatively, considering the fact that a Ge–C bond is formed, as a cyanogermyl group. This behavior is likely caused by the known reluctance of gold to engage in back-bonding, making the germylene particularly Lewis acidic and thus more likely to interact with the cyanide.

Reaction of gold complexes **3** and **4** with B(C₆F₅)₃ was attempted to abstract the phosphine ligand but only led to the formation of borane adducts **5** and **6**, where the Lewis acid coordinates to the cyanide nitrogen without altering the bonding situation in the complex significantly (Scheme 1).

Additional B(C₆F₅)₃ caused no further effect, and even heating to 100 °C for 18 h did not affect the Au–P bond according to NMR spectroscopic analysis. One property that changed, however, was light sensitivity. While solutions of complexes **3** and **4** decomposed under the influence of daylight within a few hours, solutions of the borane adducts **5** and **6** were found to be stable for weeks.

Reaction of the PEt₃-stabilized germylene **1** with silver triflate in benzene or dichloromethane caused precipitation of metallic silver and the formation of a number of decomposition products. The same reaction with silver cyanide, however, proceeded like the reactions with gold cyanide to yield the silver complex **7** as colorless crystals (Scheme 1). Compared to the gold complex **3**, the analogous silver complex was found to be more light-sensitive. Although the brownish decomposition products could easily be removed by filtration over Celite, only a few minutes in daylight produced a color change, indicating further decomposition. The molecular structure of **7** in the solid state is very similar to that of **3**; however, dimerization was

observed, which is caused by coordination of the cyanide nitrogen to the silver atom of a second complex. This leads to the formation of a dinuclear complex featuring an eight-membered ring.

Moving to copper required a change of the reaction conditions. While the reaction of germylene adduct **1** with copper cyanide in benzene resulted in the formation of the expected copper complex (**8**) analogous to **3** and **7**, the reaction was not as clean and gave a number of byproducts. Changing to THF as a solvent proved to be a viable alternative for the clean formation of **8**. Again the reaction needed to be carried out under exclusion of light. While complex **8** in the solid state is again colorless, the reaction solution is green, which may indicate the presence of Cu(II) ions. Exposure to light causes very fast color change to brown and eventually the formation of a copper mirror. The structure of complex **8** resembles the silver complex **7**, being dimeric in the solid state. In analogy to the reactions of gold complexes **3** and **4** also the silver and copper complexes **7** and **8** were treated with $B(C_6F_5)_3$ and yielded the respective borane adducts **9** and **10** (Scheme 1).

The obtained results with germylenes **1** and **2** encouraged us to extend our efforts to stannylenes. Stannylene adduct **11**¹⁸ was thus reacted with gold cyanide and subsequently with $B(C_6F_5)_3$ (Scheme 2) to show analogous reactivity resulting in the formation of complexes **12** and **13**.

NMR Spectroscopy. Unfortunately, there are no germanium isotopes with favorable NMR spectroscopic properties. However, the obtained germylene complexes (**3**–**10**) contain a number of other NMR-active nuclei (1H , ^{11}B , ^{13}C , ^{19}F , ^{29}Si , ^{31}P , $^{107/109}Ag$) (Table 1) for proper characterization and some insight into the electronic nature of the interaction between the germylene and the coinage metals. As proton and carbon chemical shifts of the backbone of the germylene and the phosphine ligand are not very characteristic, the respective spectra contain mainly information about symmetry properties.

Comparison of the ^{29}Si NMR spectra of starting material **1**¹⁹ and the respective gold complex **3** features a downfield shift of the ^{29}Si resonance of the germylene-attached silicon atoms from -127 ppm to -110 ppm. For compound **1** at ambient temperature the observed $SiMe_3$ signals are very broad (at -7.9 ppm), as they are in the coalescence regime, indicating configurational flexibility of the germanium atom.¹⁹ In contrast complex **3** shows face differentiation of the cyclic germylene with chemical shifts for two $SiMe_3$ resonances of -5.6 and -8.4 ppm. The chemical shifts of the $SiMe_2$ groups of **1** and **3** reflect their more remote position, as they are very much comparable (Table 1). If the ^{29}Si chemical shifts of **1** and **3** are considered to be comparable, the differences between those of **3** and its borane adduct **5** are almost negligible (Table 1). Supposedly, coordination of $B(C_6F_5)_3$ to the nitrile substituent is not really affecting the electronic situation of the germylene unit. At the same time ^{19}F and ^{11}B resonances of **5** are only marginally different from the simple $B(C_6F_5)_3$ -acetonitrile complex,²² again indicating minimal interaction of the borane with the metal complex. This NMR-spectroscopic picture is in essence also true for the other borane adducts **6**, **9**, **10**, and **13**.

Compared to the starting materials **1** ($\delta = 14.8$ ppm) and **2** ($\delta = 15.0$ ppm) and also to Et_3PAuCN ($\delta = 35.4$ ppm)²³ the ^{31}P resonances of gold complexes **3**, **4**, and **12** are shifted downfield to values between 48.8 and 51.0 ppm. For complexes **7** and **9** it would be attractive to obtain ^{107}Ag or ^{109}Ag NMR spectra. Although both isotopes are spin 1/2 nuclei with high

abundance, silver NMR is not very common.²⁴ The main reasons for this are very low observation frequencies, long relaxation times, and most importantly a receptivity that is about 5 orders of magnitude lower than for 1H . Nevertheless, indirect observation of ^{107}Ag and ^{109}Ag via coupling is well known. For silver halide phosphine complexes a relationship between the number of coordinating phosphines and the $^{107/109}Ag$ – ^{31}P coupling constant was established.^{25–27} Much less is known about the $^{107/109}Ag$ – ^{31}P coupling of silver phosphine complexes with heavier group 14 ligands. Older work by Sanghani et al. points out that the complex $(Ph_3P)_3AgSnCl_3$ does not feature a Sn–Ag bond in solution but is better described as $Ag(PPh_3)_3^+SnCl_3^-$.²⁸ Gade and co-workers pointed out for an $R_3SnAg(PPh_3)_n$ ($n = 1, 2$) complex that the $^{107/109}Ag$ – ^{31}P coupling for dicoordinate silver complexes is much larger than for related tricoordinate ones.²⁹ For complexes **7** and **9** of the current study the situation seems to be similar. For complex **7** no $^{107/109}Ag$ – ^{31}P coupling could be observed at ambient temperature. At -30 °C the signal became a broad doublet with a coupling constant of 360 Hz, not showing resolved coupling to the two different silver nuclei. Such behavior might be attributed to dynamic coordination change in solution.³⁰ Complex **9**, on the other hand, where the nitrile nitrogen is blocked by strong borane coordination, cannot dimerize in solution, and accordingly, even at ambient temperature $^{107/109}Ag$ – ^{31}P couplings of 366 and 433 Hz were observed in the ^{31}P NMR spectrum.

Further information about the molecular size of **7** in solution was obtained from 2D DOSY diffusion measurements on a sample containing **7** and **9** in C_6D_6 . An overlay of a regular and a proton–proton-decoupled DOSY spectrum is shown in Figure S1. Due to signal overlap, the regular DOSY spectrum contains strong tailing artifacts, which are almost completely removed in the decoupled DOSY. For both **7** and **9** similar diffusion coefficients D around -9.05 ($\log(m^2/s)$) corresponding to $9.1 \times 10^{-10} m^2/s$ were found. The hydrodynamic radius can be calculated from D using the diffusion coefficient and radius of another solution component for referencing. For this purpose we used the residual benzene signal, which is found at $D = -8.6$ ($\log(m^2/s)$), corresponding to $2.5 \times 10^{-9} m^2/s$. On the basis of the Stokes–Einstein equation, the relative hydrodynamic radii of two components are related to the diffusion coefficients by $D_1/D_2 = r_2/r_1$. The experimental diffusion coefficients of benzene and **7** and a hydrodynamic diameter of benzene of ~ 7.2 Å yield a hydrodynamic diameter for **7** (and also **9**) around 19 Å. The diameter of a dimer of **7** in the crystal structure is roughly 16 Å, which fits quite nicely to the obtained hydrodynamic diameter and is certainly above the size of the isostructural monomeric gold complex **3**, with a diameter of ~ 12 Å. When two aggregation states are in equilibrium, the NMR-derived diffusion coefficient is more influenced by the smaller/faster diffusing component. This indicates that in the monomer–dimer equilibrium of **7** the dimer is the predominant form.

The picture of the ^{29}Si NMR spectra of silver complexes **7** and **9** resembles that of the respective gold complexes **3** and **5** (Table 1). While the chemical shifts of the germanium-attached silicon atoms of the silver complexes (**7**, **9**) are slightly moved to higher field compared to the gold complexes (**3**, **5**), the ^{29}Si spectra of the silver complexes (**7**, **9**) and their respective copper analogues (**8**, **10**) are almost identical (Table 1).

As found for the germylene complexes, the ^{29}Si , ^{13}C , and 1H NMR spectra of the stannylene gold complexes **12** and **13**

indicated a symmetric stannacyclopentasilane with face differentiation (i.e., two sets of trimethylsilyl and methyl groups). The situation is very similar to the germylene cases of **3** and **4**. ^{29}Si NMR resonances of the **12** and **13** are shifted somewhat to lower field compared to the stannylene adduct **11** (Table 1). ^{29}Si NMR chemical shifts of the SiMe_3 , and SiMe_2 resonances of **11**, **12**, and **13** are almost identical. Not unexpected also ^{31}P shifts of **12** and **13** are close to those of **3** and **5**. Complex **12** exhibits a doublet at -126 ppm in the ^{119}Sn NMR spectrum with a P–Sn coupling constant of 1581 Hz, suggesting that it possesses a very low degree of stannylene character and might rather be considered as a stannyl complex. Again, the fact that the cyanide ion is coordinated to the tin atom indicates that the stannylene serves mainly as a σ -donor to gold and that the extent of back-donation from the gold atom to tin is very small. This behavior is certainly consistent with the rather common chemical shifts for the tin atoms. The face differentiation visible in the NMR spectra further indicates that the interaction between the stannylene and the cyanide is not limited to the solid state.

X-ray Crystallography. Most of the complexes studied in this account could be characterized by X-ray single-crystal structure diffraction analysis. The thus obtained structural data allow comparison of compounds containing gold, silver, and copper complexes, germylene and stannylene ligands, and $\text{B}(\text{C}_6\text{F}_5)_3$ adducts of these complexes. Basic structural data are compiled in Table 2.

The number of reported solid-state structures containing bonds between heavy group 14 atoms and coinage metals is not very high. If cluster compounds are excluded, a rather small number emerges. A search in the Cambridge Crystallographic Database (CCDC)³¹ reveals Ge–Au distances for complexes with dicoordinate gold between 2.324 and 2.423 Å.^{9,10,32–37} For Ge–Ag the distance range is 2.412–2.467 Å,^{8,34,38–42} for Ge–Cu a range of 2.287–2.376 Å^{42–47} was found for tetracoordinate Ge (i.e., germyl groups or base-stabilized germylens), and two values of 2.214 and 2.249 Å were reported for bonds between non-base-stabilized germylene ligands and copper.¹² For the distance Sn–Au with dicoordinate gold again only a few examples are known with a reported Sn–Au range of 2.565–2.614 Å.^{10,48} Compounds **3** (Figure 1) and **4** (Figure S2), which crystallize in the monoclinic space group $P2(1)/c$, are isotypic and feature two independent molecules in the asymmetric unit. The Ge–Au distances, which are between 2.398 and 2.429 Å, are at the longer end of the mentioned range. Complexes **5** (Figure 2) and **6** (Figure S3), being the $\text{B}(\text{C}_6\text{F}_5)_3$ adducts of **3** and **4**, crystallize in the orthorhombic space group $\text{Pna}2(1)$. They exhibit Ge–Au distances of 2.417 and 2.415 Å. In accordance with the discussed NMR data, these values show that the Ge–Au interaction is essentially not affected by the coordination of the borane. The same is also true for the Au–P distances of complexes **3–6**, which range between 2.298 and 2.320 Å. Not even the bond between the germanium and the nitrile carbon displays much variation comparing complexes **3** and **4** to **5** and **6** (Table 2). The only distinct structural difference between the core structures of these two types of molecules is the Au–Ge–CN angle. While rather typical tetrahedral angle values of 104° and 108° were found for complexes **3** and **4**, this angle is somewhat diminished to values close to 97° for complexes **5** and **6**. Due to the higher steric demand of the $\text{B}(\text{C}_6\text{F}_5)_3$ unit, the nitrile groups are bent away to avoid interaction with the trimethylsilyl groups. All complexes **3–6** feature an almost

Table 2. Compilation of Structural Data Derived by Single-Crystal XRD Analysis

compound	$d_{\text{M-E}}$	$d_{\text{M-P}}$	$d_{\text{E-C}}$	$D_{\text{E-Si}}$	$d_{\text{E-N}}$	\angle_{MEC}	\angle_{EMP}	\angle_{EEE}
3	2.402(1)/2.428(1)	2.312(3)/2.314(4)	2.01(1)/1.98(1)	2.416(3)/2.416(3)/2.415(3)/2.413(2)	n.a.	104.3(3)/108.0(3)	177.28(8)/175.7(1)	106.47(9)/107.7(1)
4	2.4292(9)/2.3981(9)	2.320(3)/2.315(2)	1.980(6)/2.023(7)	n.a.	n.a.	108.2(2)/104.8(2)	175.70(7)/177.28(5)	107.31(3)/106.16(3)
5	2.4165(5)	2.2979(9)	2.005(3)	2.410(1)/2.406(1)	1.564(4)	97.09(8)	176.50(2)	110.29(3)
6	2.4145(8)	2.303(2)	2.018(5)	n.a.	1.582(7)	97.1(2)	176.61(4)	110.08(3)
7	2.4848(8)	2.427(3)	1.986(5)	2.423(2)/2.427(2)	n.a.	107.9(2)	156.65(8)	104.51(5)
8	2.379(2)	2.228(3)	1.989(9)	2.428(3)/2.425(3)	n.a.	100.9(3)	142.5(1)	102.56(9)
10	2.3166(5)	2.2011(8)	1.998(2)	2.4103(8)/2.4134(8)	1.575(3)	98.02(6)	176.98(2)	108.43(2)
12	2.5867(6)/2.5713(6)	2.314(2)/2.311(2)	2.179(4)/2.208(7)	2.592(2)/2.588(2)	n.a.	109.2(1)/105.9(2)	174.83(5)/176.91(4)	104.91(5)/103.71(5)
13	2.5755(7)	2.307(1)	2.241(3)	2.583(1)/2.589(1)	1.573(4)	103.27(9)	177.67(3)	105.32(3)

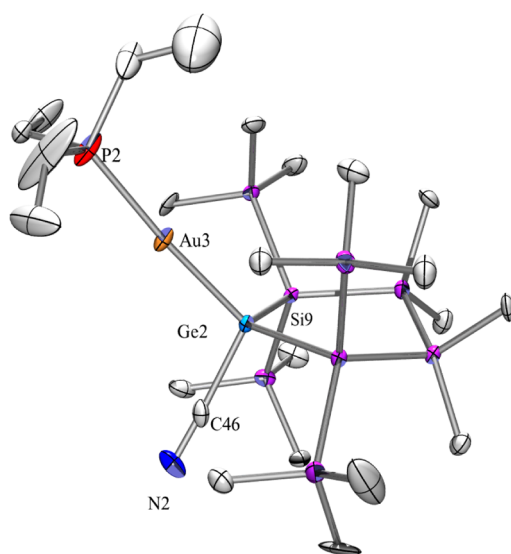


Figure 1. Crystal structure of **3**. Displacement ellipsoids are represented at the 30% level, and hydrogen atoms have been omitted for clarity (bond lengths in Å, angles in deg): Au(3)–P(2) 2.314(3), Au(3)–Ge(2) 2.4277(11), C(46)–N(2) 1.147(13), C(46)–Ge(2) 1.978(12), C(1)–Si(2) 1.882(10), C(2)–Si(2) 1.876(11), C(42)–P(2) 1.813(11), Ge(2)–Si(9) 2.416(3), Si(9)–Si(10) 2.349(4), P(2)–Au(3)–Ge(2) 175.68(11), N(2)–C(46)–Ge(2) 176.6(10), C(46)–Ge(2)–Si(9) 102.6(3), Si(12)–Ge(2)–Si(9) 107.68(10), C(46)–Ge(2)–Au(3) 107.9(3), Si(9)–Ge(2)–Au(3) 115.60(7).

linear Ge–Au–P arrangement with respective angles between 176° and 178° .

In contrast to the gold complexes **3** and **4**, the respective silver and copper complexes **7** (Figure S4) and **8** (Figure 3), which are again isotypic and crystallize in the monoclinic space group $P2(1)/n$, are dimeric in the solid state. The dimerization occurs by coordination of the nitrile nitrogen to the respective metal of a second complex unit. The copper and silver atoms are thus tricoordinate and the Ge–M–P angles are 158° and 142° for M = Ag and Cu, respectively. Once the dimerization is inhibited by coordination of $B(C_6F_5)_3$ to the nitrile nitrogen atom, the Ge–Cu–P angle of the copper complex **10** (Figure S5) is restored to an almost linear fashion of 178° . The dimeric structures of **7** and **8** represent eight-membered rings that are almost completely flat. As the Ge–C–N unit is close to linear, the appearance of the rings is that of distorted hexagons. The Ag–Ge distance of **7** of 2.4848(8) Å is comparably long. While the complex geometry of the gold complexes **3** and **4** and their respective borane adducts **5** and **6** was almost identical, there are quite remarkable differences between the dimeric copper complex **8** and its borane adduct **10**. The most striking difference is seen in the Cu–Ge bond length, which at 2.379(2) Å for the dimeric complex **8** is rather long but is shortened to 2.3166(5) Å for the monomeric complex **10**. Also the Cu–P bond follows this trend; however, not to the same extent, as the bond length shortens from 2.228(3) Å for **8** to 2.2011(8) Å for **10**. It seems likely that the bond elongation of the dimeric complex is related to the tricoordinate bonding situation at copper and the rather strong distortion of linearity of the Ge–Cu–P unit.

The structural situation of the tin-containing gold complexes **12** (Figure 4) and **13** (Figure S6) is very similar to that of **3/4** and **5/6**. Complex **12** is isotypic to **3/4** and therefore has two independent complexes in the asymmetric unit. The Sn–Au

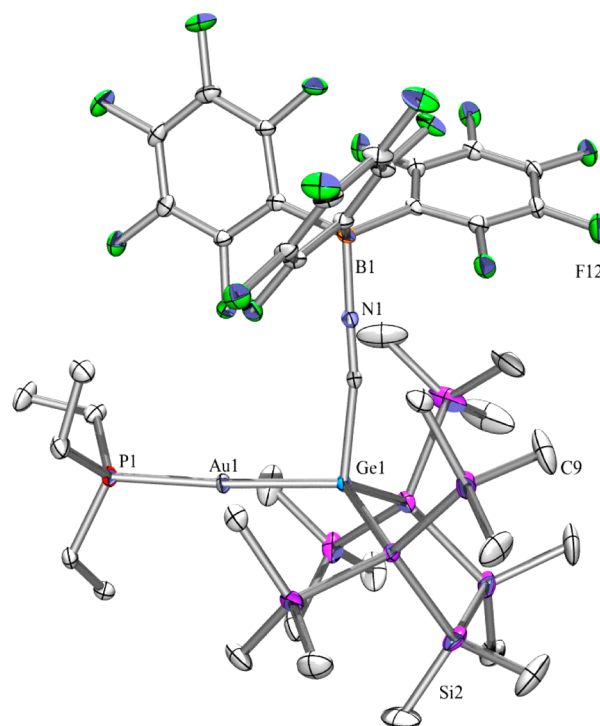


Figure 2. Crystal structure of **5**. Displacement ellipsoids are represented at the 30% level, and hydrogen atoms have been omitted for clarity (bond lengths in Å, angles in deg): Au(1)–P(1) 2.2979(9), Au(1)–Ge(1) 2.4165(5), Ge(1)–C(41) 2.005(3), Ge(1)–Si(4) 2.4064(11), Ge(1)–Si(1) 2.4100(11), N(1)–C(41) 1.147(4), N(1)–B(1) 1.564(4), P(1)–C(17) 1.816(3), Si(1)–Si(2) 2.3407(13), Si(2)–C(1) 1.896(5), B(1)–C(35) 1.640(4), F(1)–C(24) 1.357(4), P(1)–Au(1)–Ge(1) 176.50(2), C(41)–Ge(1)–Si(4) 106.54(8), C(41)–Ge(1)–Si(1) 106.74(9), Si(4)–Ge(1)–Si(1) 110.29(4), C(41)–Ge(1)–Au(1) 97.09(8), Si(4)–Ge(1)–Au(1) 118.44(3), Si(1)–Ge(1)–Au(1) 115.74(3).

bond distance, at 2.587/2.571 Å, is in the expected region. In the same way complex **13** is isotypic to **5/6**. Again the only major structural difference of the core structures of **12** and **13** is the Au–Sn–CN angle, which is smaller for **13** for the same reasons as outlined above.

The question whether the complexes described in this study can be considered as cyanide adducts of germylene (Ge(II)) complexes or as cyanogermyl (Ge(IV)) complexes may be answered by a comparison of already known structures containing the germacyclopentasilane motif containing either Ge(II) or Ge(IV). Evaluation of the Si–Ge bond distances reveals that this parameter is quite sensitive to the oxidation state of the Ge atom. While the PEt_3 and NHC germylene adducts¹⁹ feature distances of 2.477 and 2.471 Å, respectively, for the corresponding dimethylgermylene compound,⁴⁹ only a distance of 2.408 Å was found. The Si–Ge bond distances of 2.475, 2.465, and 2.455 Å found for the germylene complexes of titanocene, zirconocene, and hafnocene²¹ indicate these complexes having germylene character, which diminishes in the shown order. If we use these values as a basis for assigning the oxidation states of complexes **3**, **5**, **7**, **8**, and **10**, we find distances between 2.406 and 2.414 Å for the gold complexes **3** and **5**, distances of 2.426 and 2.427 Å for the silver complex **7**, and distances between 2.410 and 2.428 Å for the copper complexes **9** and **10** (Table 2). All these values certainly assign the Ge atom an oxidation number of IV. Therefore, it seems

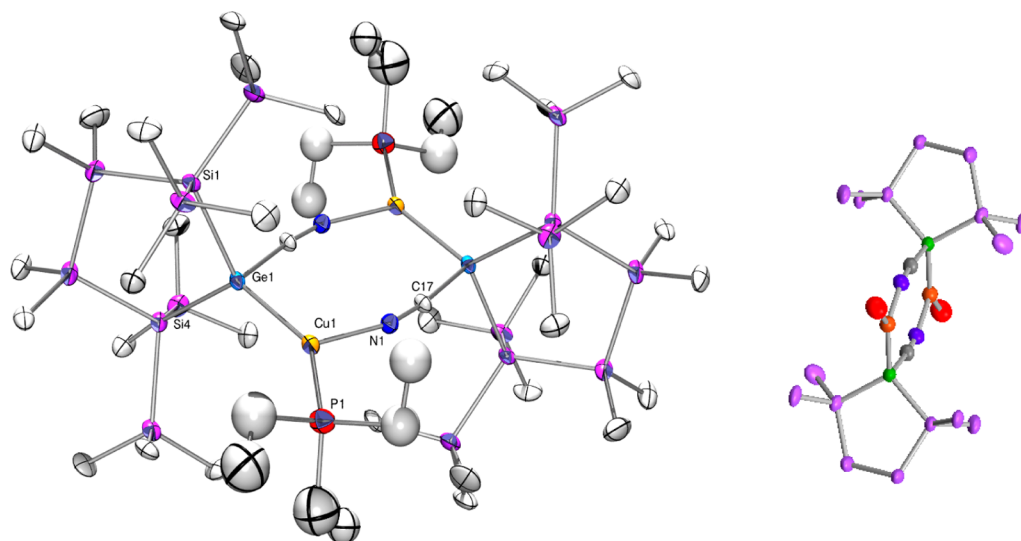


Figure 3. Crystal structure of **8**. Left side: displacement ellipsoids are represented at the 30% level and hydrogen atoms have been omitted for clarity (bond lengths in Å, angles in deg). Cu(1)–N(1) 2.006(8), Cu(1)–P(1) 2.228(3), Cu(1)–Ge(1) 2.3788(16), Ge(1)–C(17-1) 1.989(9), Ge(1)–Si(1) 2.428(3), N(1)–C(17) 1.141(10), P(1)–C(18) 1.839(9), Si(1)–Si(2) 2.340(4), Si(2)–C(2) 1.848(14), N(1)–Cu(1)–Ge(1) 105.7(2), C(17-1)–Ge(1)–Cu(1) 100.9(3), C(17)–N(1)–Cu(1) 162.0(8), N(1)–C(17)–Ge(1-1) 171.2(8). Right side: hydrogen and carbon atoms have been omitted for clarity.

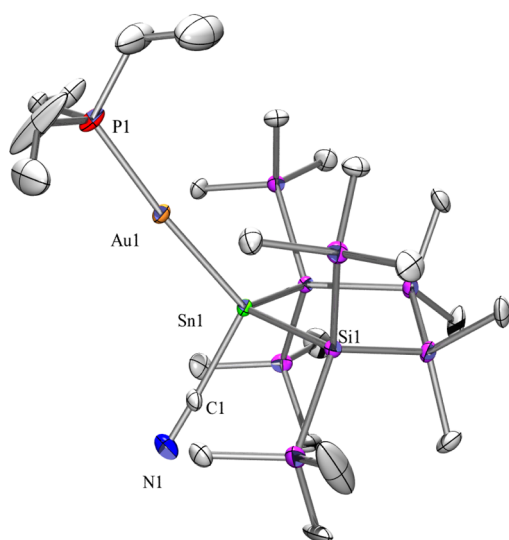


Figure 4. Molecular structure of **12** (displacement ellipsoid plot drawn at the 30% probability level). Hydrogen atoms are omitted for clarity (bond lengths in Å, angles in deg): Au(1)–P(1) 2.314(3), Au(1)–Sn(1) 2.5876(8), Sn(1)–C(1) 2.181(10), Sn(1)–Si(4) 2.588(3), Sn(1)–Si(1) 2.590(3), Si(1)–Si(6) 2.346(4), Si(2)–C(4) 1.886(11), P(1)–C(19) 1.813(12), C(1)–N(1) 1.143(13), P(1)–Au(1)–Sn(1) 174.74(9), C(1)–Sn(1)–Au(1) 109.3(2), Au(1)–Sn(1)–Si(1) 118.43(6), Si(4)–Sn(1)–Si(1) 104.99(8), N(1)–C(1)–Sn(1) 177.6(9).

more appropriate to consider these compounds as cyanogermyl complexes. The same type of analysis carried out for structures containing the stannacyclopentasilane leads to analogous conclusions. The PET_3 adduct of the cyclic five-membered stannylene features Si–Sn bond distances of 2.653 Å,¹⁸ whereas the related bond in the diphenylstannylene compound⁵⁰ is as short as 2.594 Å. Again the Si–Sn bond distances found for **12** (2.592(2)/2.588(2)) and **13** (2.583(1)/2.589(1)) (Table 2) are clearly indicative of cyanostannyl ligands.

A similar analysis of the Ge–CN and Sn–CN bonds is not as straightforward. The number of structurally characterized cyanogermanes^{51–54} and cyanostannanes^{54,55} is very small. However, given a Ge–CN distance of 1.975(11) Å for Mes_3GeCN ,⁵² the range of 1.98 to 2.02 Å found for the Ge–CN distance in complexes **3–8** and **10** is quite comparable and points at a regular covalent bond. Although the structure of Me_3SnCN is known and a Sn–CN distance of 2.295(12) Å was found, the value is likely not very representative, as Me_3SnCN exists as a coordination polymer with hypercoordinated tin atoms in the solid state.⁵⁵ As the quality of the structure of $\text{Me}_2\text{Sn}(\text{CN})_2$ (with a Sn–CN distance of 2.27(7) Å)⁵⁴ is not very good, the values between 2.179(4) and 2.241(3) Å for complexes **12** and **13** also are indicative of regular covalent Sn–C bonds.

3. CONCLUSION

Using the Et_3P adducts of bissilylated germynes and stannylenes as starting materials, reactions with gold, silver, and copper cyanides led to cyanogermyl or -stannyl phosphine complexes of the respective metals. In the reaction process the cyanide and phosphine ligands were exchanged. While solid-state structures of gold complexes displayed the well-known linear coordination geometry, the silver and copper complexes were found to exist as dimers in the solid state with the nitrile serving as the bridging unit, which coordinates with the nitrogen atom to the metal of a neighboring complex. As a result of the dimerization, the silver and copper atoms are tricoordinate, with the dimer forming a hexagonally shaped eight-membered ring. The deviation from the linear coordination mode characterized by the E–M–P angle is much stronger for copper (142°) than for silver (158°). Subsequent reactions of the obtained complexes with $\text{B}(\text{C}_6\text{F}_5)_3$ led to the formation of adducts with the borane coordinating to the cyanide nitrogen atom. The formation of the borane adduct also causes a restoration of the linear coordination mode. With respect to NMR spectroscopic and structural properties there are almost negligible differences between the free complexes and their

borane adducts, with the exception of the copper complexes. Supposedly, the interaction between the copper atom and the germylene is stronger in the dimeric case.

In principle all observed complexes can be seen either as cyanide adducts of metal ylenc complexes with Ge(II) or Sn(II) ligands or as cyanogermyl or -stannyl complexes with tetravalent Ge(IV) and Sn(IV). A thorough comparison of the structural parameters of the five-membered rings showed explicit indication for classifying these complexes as cyanogermyl and -stannyl complexes. This assignment is further strengthened by ^{119}Sn NMR spectroscopic analysis.

4. EXPERIMENTAL SECTION

General Remarks. All reactions involving air-sensitive compounds were carried out under an atmosphere of dry nitrogen or argon using either Schlenk techniques or a glovebox. All solvents were dried using a column-based solvent purification system.⁵⁶ Phosphine-stabilized germylenes **1**¹⁹ and **2**¹⁹ and phosphine-stabilized stannylene **11**¹⁸ were prepared according to published procedures. All other chemicals were obtained from different suppliers and used without further purification.

^1H (300 MHz), ^{13}C (75.4 MHz), ^{29}Si (59.3 MHz), ^{31}P (124.4 MHz), ^{11}B (96.0 MHz), ^{19}F (282.2 MHz), and ^{119}Sn (111.8 MHz) NMR spectra were recorded on a Varian INOVA 300 spectrometer. If not noted otherwise for all samples, benzene- d_6 was used as solvent, or in the case of reaction samples they were measured with a water- d_2 capillary in order to provide an external lock frequency signal. To compensate for the low isotopic abundance of ^{29}Si , the INEPT pulse sequence was used for the amplification of the signal.^{57,58} To obtain self-diffusion coefficients, two-dimensional diffusion ordered spectroscopy (DOSY) was used.⁵⁹ The employed pulse sequence was a bipolar pulse pair longitudinal eddy current delay (BPP-LED) sequence, using 32 scans per increment, 60 ms diffusion delay time, 1 ms gradient pulses, and variation of the gradient strength in 32 increments, linearly varied between 2% and 95% of maximum (which is 53.5 G/cm). DOSY analysis was performed using the Bruker DOSY package of TopSpin 3.1. Due to extensive signal overlap, also an instant homonuclear broadband-decoupled 2D DOSY spectrum was acquired.⁶⁰ For this experiment 128 scans were recorded per increment, and for proton–proton decoupling a 10 ms 180° Gaussian pulse during a 0.5 G/cm slice-selection gradient was used. Fifty data chunks of 27 ms were acquired, amounting to a total acquisition time of 1.35 s. All other parameters were the same as used for the regular DOSY. All DOSY measurements were carried out at 300 K on a Bruker Avance III 500 MHz NMR spectrometer using a 5 mm TXI probe with z-axis gradients.

Elementary analysis was carried out using a Heraeus Vario Elementar. Due to SiF_4 formation in the combustion of $\text{B}(\text{C}_6\text{F}_5)_3$ adducts, no elemental analyses were determined for these compounds.

X-ray Structure Determination. For X-ray structure analyses the crystals were mounted onto the tip of glass fibers, and data collection was performed with a Bruker-AXS SMART APEX CCD diffractometer using graphite-monochromated Mo $K\alpha$ radiation (0.710 73 Å). The data were reduced to F_o^2 and corrected for absorption effects with SAINT⁶¹ and SADABS,⁶² respectively. The structures were solved by direct methods and refined by full-matrix least-squares method (SHELXL97).⁶³ If not noted otherwise, all non-hydrogen atoms were refined with anisotropic displacement parameters. All hydrogen atoms were located in calculated positions to correspond to standard bond lengths and angles. All diagrams were drawn with 30% probability displacement ellipsoids, and all hydrogen atoms were omitted for clarity. Crystallographic data (excluding structure factors) for the structures of compounds **3**, **4**, **5**, **6**, **7**, **8**, **10**, **12**, and **13** reported in this paper have been deposited with the Cambridge Crystallographic Data Center as supplementary publication nos. CCDC-936049 (**3**), 936047, (**4**), 936048 (**5**), 936052 (**6**), 936050 (**7**), 936053 (**8**), 943915 (**10**), 936046 (**12**), and 971935 (**13**) and can be obtained free of charge at <http://www.ccdc.cam.ac.uk/products/csd/request/>.

Triethylphosphino[2-cyano-2-germa-1,1,3,3-tetrakis(trimethylsilyl)tetramethylcyclopentasilan-2-yl]gold(I) (3). AuCN (22 mg, 0.10 mmol) and **1** (66 mg, 0.10 mmol) were dissolved in benzene (2 mL). After stirring for 12 h at rt. NMR control measurement showed complete conversion. The solvent was removed, and the remaining off-white residue was diluted with toluene/pentane (1:1) and filtrated through glass wool. After storage at -30°C colorless crystals of **3** (37 mg, 43%) were obtained. Mp: 190–192 °C (dec). ^1H NMR (δ ppm): 1.10 (m, 6H, PCH_2CH_3), 0.77 (m, 9H, CH_2CH_3), 0.62 (s, 18H, Me_3Si), 0.52 (s, 6H, Me_2Si), 0.46 (s, 18H, Me_3Si), 0.42 (s, 6H, Me_2Si). ^{13}C NMR (δ ppm): 132.1 (d, $^3J_{\text{C,P}} = 1$ Hz, CN), 18.1 (d, $^1J_{\text{C,P}} = 26$ Hz, PCH_2CH_3), 8.7 (CH_2CH_3), 3.5 (Me_3Si), 3.1 (Me_3Si), -1.4 (Me_2Si), -1.6 (Me_2Si). ^{29}Si NMR (δ ppm): -5.6 (Me_3Si), -8.4 (Me_3Si), -21.4 (d, $^4J_{\text{Si,P}} = 5$ Hz, Me_2Si), -110.4 (d, $^3J_{\text{Si,P}} = 7$ Hz, Si_q). ^{31}P NMR (δ ppm): 49.0. Anal. Calcd for $\text{C}_{23}\text{H}_{63}\text{AuGeNPSi}_8$ (879.02): C 31.43, H 7.22, N 1.59. Found: C 32.04, H 7.17, N 1.62.

Triethylphosphino[2-cyano-1,2,3-trigerma-1,1,3,3-tetrakis(trimethylsilyl)tetramethylcyclopentasilan-2-yl]gold(I) (4). Reaction was done according to procedure for **3** using AuCN (44 mg, 0.20 mmol) and **2** (149 mg, 0.20 mmol). Colorless crystals of **3** (121 mg, 63%) were obtained. Mp: 188–189 °C (dec). ^1H NMR (δ ppm): 1.11 (m, 6H, PCH_2CH_3), 0.78 (m, 9H, CH_2CH_3), 0.64 (s, 18H, Me_3Si), 0.54 (s, 6H, Me_2Si), 0.49 (s, 18H, Me_3Si), 0.44 (s, 6H, Me_2Si). ^{13}C NMR (δ ppm): 133.6 (d, $^3J_{\text{C,P}} = 2$ Hz, CN), 18.2 (d, $^1J_{\text{C,P}} = 26$ Hz, PCH_2CH_3), 8.7 (CH_2CH_3), 4.1 (Me_3Si), 3.7 (Me_3Si), -0.8 (Me_2Si), -1.0 (Me_2Si). ^{29}Si NMR (δ ppm): 0.2 (Me_3Si), -3.7 (Me_3Si), -15.3 (d, $^4J_{\text{Si,P}} = 5.1$ Hz, Me_2Si). ^{31}P NMR (δ ppm): 48.8. Anal. Calcd for $\text{C}_{23}\text{H}_{63}\text{Ge}_3\text{NPSi}_6$ (968.13): C 28.53, H 6.56, N 1.45. Found: C 28.71, H 6.41, N 2.00.

Triethylphosphino[2-cyano-2-germa-1,1,3,3-tetrakis(trimethylsilyl)tetramethylcyclopentasilan-2-yl]gold(I)- $\text{B}(\text{C}_6\text{F}_5)_3$ (5). Tris(pentafluorophenyl)borane (25 mg, 0.050 mmol) and **3** (44 mg, 0.050 mmol) were dissolved in benzene (2 mL). After stirring for 30 min at rt, NMR control measurement showed complete conversion. The solvent was removed, and the remaining off-white residue was diluted with pentane and filtrated through glass wool. After storage at -30°C colorless crystals of **5** (23 mg, 33%) were obtained. Mp: 171–173 °C (dec). ^1H NMR (δ ppm): 1.22 (m, 6H, PCH_2CH_3), 0.83 (m, 9H, CH_2CH_3), 0.38 (s, 18H, Me_3Si), 0.31 (s, 6H, Me_2Si), 0.25 (s, 6H, Me_3Si), 0.17 (s, 18H, Me_3Si). ^{11}B NMR (δ ppm): -11.5 . ^{13}C NMR (δ ppm): 149.1 (dm, $^1J_{\text{F,C}} = 238$ Hz, CF), 140.9 (dm, $^1J_{\text{F,C}} = 250$ Hz, CF), 138.2 (CN), 138.0 (dm, $^1J_{\text{F,C}} = 249$ Hz, CF), 118.1 (m, CB), 18.1 (d, $^1J_{\text{C,P}} = 27$ Hz, PCH_2CH_3), 8.3 (CH_2CH_3), 3.1 (Me_3Si), 2.2 (Me_3Si), -1.7 (Me_2Si), -2.2 (Me_2Si). ^{19}F NMR (δ ppm): -132.2 (dd, $^3J_{\text{F,F}} = 24$ Hz, $^4J_{\text{F,F}} = 8$ Hz, $o\text{-ArF}$), -158.0 (t, $^3J_{\text{F,F}} = 21$ Hz, $p\text{-ArF}$), -164.4 (dt, $^3J_{\text{F,F}} = 24$ Hz, $^4J_{\text{F,F}} = 9$ Hz, $m\text{-ArF}$). ^{29}Si NMR (δ ppm): -5.5 (d, $^4J_{\text{Si,P}} = 2$ Hz, Me_3Si), -7.9 (Me_3Si), -23.2 (d, $^4J_{\text{Si,P}} = 3$ Hz, Me_2Si), -110.0 (d, $^3J_{\text{Si,P}} = 6$ Hz, Si_q). ^{31}P NMR (δ ppm): 47.5.

Triethylphosphino[2-cyano-1,2,3-trigerma-1,1,3,3-tetrakis(trimethylsilyl)tetramethylcyclopentasilan-2-yl]gold(I)- $\text{B}(\text{C}_6\text{F}_5)_3$ (6). Reaction was done according to the procedure for **5** using tris(pentafluorophenyl)borane (26 mg, 0.050 mmol) and **4** (48 mg, 0.050 mmol). Colorless crystals of **6** (36 mg, 52%) were obtained. Mp: 161–165 °C (dec). ^1H NMR (δ ppm): 1.21 (m, 6H, PCH_2CH_3), 0.83 (m, 9H, CH_2CH_3), 0.41 (s, 18H, Me_3Si), 0.34 (s, 6H, Me_2Si), 0.29 (s, 6H, Me_3Si), 0.21 (s, 18H, Me_3Si). ^{11}B NMR (δ ppm): -11.9 . ^{13}C NMR (δ ppm): 149.1 (dm, $^1J_{\text{F,C}} = 238$ Hz, CF), 140.9 (dm, $^1J_{\text{F,C}} = 250$ Hz, CF), 139.6 (CN), 138.1 (dm, $^1J_{\text{F,C}} = 249$ Hz, CF), 118.2 (m, CB), 18.1 (d, $^1J_{\text{C,P}} = 26$ Hz, PCH_2CH_3), 8.3 (CH_2CH_3), 3.7 (Me_3Si), 2.8 (Me_3Si), -1.1 (Me_2Si), -1.6 (Me_2Si). ^{19}F NMR (δ ppm): -132.3 (dd, $^3J_{\text{F,F}} = 24$ Hz, $^4J_{\text{F,F}} = 8$ Hz, $o\text{-ArF}$), -158.2 (t, $^3J_{\text{F,F}} = 21$ Hz, $p\text{-ArF}$), -164.4 (dt, $^3J_{\text{F,F}} = 24$ Hz, $^4J_{\text{F,F}} = 9$ Hz, $m\text{-ArF}$). ^{29}Si NMR (δ ppm): 0.8 (d, $^4J_{\text{Si,P}} = 3$ Hz), -2.6 , -16.3 (d, $^4J_{\text{Si,P}} = 3$ Hz). ^{31}P NMR (δ ppm): 47.6.

Triethylphosphino[2-cyano-2-germa-1,1,3,3-tetrakis(trimethylsilyl)tetramethylcyclopentasilan-2-yl]silver(I) (7). Reaction was done according to the procedure for **3** using AgCN (13 mg, 0.10 mmol) and **2** (66 mg, 0.10 mmol). Reaction control by NMR showed complete conversion after 1 h. Colorless crystals of **7** (57 mg,

72%) were obtained. Mp: 156–157 °C (dec). ^1H NMR (δ ppm): 0.94 (m, 6H, PCH_2CH_3), 0.72 (m, 9H, PCH_2CH_3), 0.66 (s, 18H, Me_3Si), 0.57 (s, 6H, Me_2Si), 0.44 (s, 6H, Me_2Si), 0.43 (s, 18H, Me_3Si). ^{13}C NMR (δ ppm): 131.5 ($\text{C}\equiv\text{N}$), 16.6 (d, $^1J_{\text{C,P}} = 17$ Hz), 9.2 (d, $^2J_{\text{C,P}} = 4$ Hz, PCH_2CH_3), 3.2 (Me_3Si), 3.2 (Me_3Si), -1.4 (Me_2Si), -1.6 (Me_2Si). ^{29}Si NMR (δ ppm): -5.8 (Me_3Si), -9.0 (Me_3Si), -21.4 (Me_2Si), -114.2 (Si_q). ^{31}P NMR (δ ppm): 4.7(rt); 3.3 (-30 °C, toluene- d_6 , bd, $^1J_{\text{P,Ag}} = 360$ Hz). Anal. Calcd for $\text{C}_{23}\text{H}_{63}\text{AgGeNPSi}_8$ (789.92): C 34.97, H 8.04, N 1.77. Found: C 35.96, H 7.96, N 1.83.

Triethylphosphino[2-cyano-2-germa-1,1,3,3-tetrakis(trimethylsilyl)tetramethylcyclopentasilan-2-yl]copper(I) (8). Reaction was done according to the procedure for 3 using CuCN (10 mg, 0.10 mmol), 2 (66 mg, 0.10 mmol), and THF as solvent. Reaction was done under exclusion of light. Reaction control by NMR showed complete conversion after 1 h. Colorless, extremely light sensitive crystals of 8 (35 mg, 46%) were obtained. Mp: 148–149 °C (dec). ^1H NMR (δ ppm): 1.47 (m, 6H, PCH_2CH_3), 0.97 (m, 9H, PCH_2CH_3), 0.58 (s, 18H, Me_3Si), 0.57 (s, 6H, Me_2Si), 0.47 (s, 6H, Me_2Si), 0.42 (s, 18H, Me_3Si). ^{13}C NMR (δ ppm): CN was not detected, 16.6 (d, $^1J_{\text{C,P}} = 14$ Hz, PCH_2CH_3), 9.3 (PCH_2CH_3), 4.4 (Me_3Si), 4.1 (Me_3Si), -0.8 (Me_2Si), -1.1 (Me_2Si). ^{29}Si NMR (δ ppm): -6.6 (Me_3Si), -8.8 (Me_3Si), -22.1 (Me_2Si), -115.6 (Si_q). ^{31}P NMR (δ ppm): -16.5. Anal. Calcd for $\text{C}_{23}\text{H}_{63}\text{CuGeNPSi}_8$ (745.60): C 37.05, H 8.52, N 1.88. Found: C 38.75, H 8.38, N 1.92.

Triethylphosphino[2-cyano-2-germa-1,1,3,3-tetrakis(trimethylsilyl)tetramethylcyclopentasilan-2-yl]silver(I)-B(C₆F₅)₃ (9). Reaction was done according to the procedure for 5 using tris(pentafluorophenyl)borane (51 mg, 0.10 mmol) and 4 (79 mg, 0.10 mmol). Colorless crystals of 9 (126 mg, 97%) were obtained. Mp: 169–171 °C (dec). ^1H NMR (δ ppm): 1.08 (m, 6H, PCH_2CH_3), 0.80 (m, 9H, CH_2CH_3), 0.33 (s, 24H, $\text{Me}_3\text{Si}/\text{Me}_2\text{Si}$), 0.25 (s, 6H, Me_2Si), 0.17 (s, 18H, Me_3Si). ^{11}B NMR (δ ppm): -11.7. ^{13}C NMR (δ ppm): 148.7 (dm, $^1J_{\text{F,C}} = 241$ Hz, CF), 140.4 (dm, $^1J_{\text{F,C}} = 256$ Hz, CF), 137.8 (CN), 137.6 (dm, $^1J_{\text{F,C}} = 271$ Hz, CF), 118.0 (m, CB), 16.7 (dd, $^1J_{\text{C,P}} = 19$ Hz, $^2J_{\text{C,Ag}} = 4$ Hz, PCH_2CH_3), 9.0 (dd, $^2J_{\text{C,P}} = 3$ Hz, $^3J_{\text{C,Ag}} = 2$ Hz, CH_2CH_3), 2.6 (Me_3Si), 2.2 (Me_3Si), -1.6 (Me_2Si), -2.3 (Me_2Si). ^{19}F NMR (δ ppm): -132.8 (dd, $^3J_{\text{F,F}} = 23$ Hz, $^4J_{\text{F,F}} = 7$ Hz, *o*-ArF), -158.2 (t, $^3J_{\text{F,F}} = 20$ Hz, *p*-ArF), -164.4 (dt, $^3J_{\text{F,F}} = 24$ Hz, $^4J_{\text{F,F}} = 9$ Hz, *m*-ArF). ^{29}Si NMR (δ ppm): -5.9 (d, $^4J_{\text{Si,P}} = 3$ Hz, Me_3Si), -8.7 (d, $^4J_{\text{Si,P}} = 2$ Hz, Me_3Si), -22.7 (dd, $^4J_{\text{Si,P}} = 3$ Hz, $^3J_{\text{Si,Ag}} = 2$ Hz, Me_2Si), -114.6 (dd, $^3J_{\text{Si,P}} = 11$ Hz, $^2J_{\text{Si,Ag}} = 4$ Hz, Si_q). ^{31}P NMR (δ ppm): 7.4 (d, $^1J_{109\text{Ag,P}} = 423$ Hz, d, $^1J_{107\text{Ag,P}} = 366$ Hz).

Triethylphosphino[2-cyano-2-germa-1,1,3,3-tetrakis(trimethylsilyl)tetramethylcyclopentasilan-2-yl]copper(I)-B(C₆F₅)₃ (10). Reaction was done according to the procedure for 5 using tris(pentafluorophenyl)borane (51 mg, 0.10 mmol) and 8 (75 mg, 0.10 mmol). Colorless crystals of 9 (93 mg, 74%) were obtained. Mp: 148–150 °C (dec). ^1H NMR (δ ppm): 1.16 (m, 6H, PCH_2CH_3), 0.80 (m, 9H, CH_2CH_3), 0.30 (s, 24H, $\text{Me}_3\text{Si}/\text{Me}_2\text{Si}$), 0.23 (s, 6H, Me_2Si), 0.15 (s, 18H, Me_3Si). ^{11}B NMR (δ ppm): -11.7. ^{13}C NMR (δ ppm): 148.9 (dm, $^1J_{\text{F,C}} = 243$ Hz, CF), 140.6 (dm, $^1J_{\text{F,C}} = 256$ Hz, CF), 137.8 (dm, $^1J_{\text{F,C}} = 248$ Hz, CF), 136.9 (CN), 117.0 (m, CB), 15.6 (d, $^1J_{\text{C,P}} = 19$ Hz, PCH_2CH_3), 8.4 (CH_2CH_3), 3.0 (Me_3Si), 2.2 (Me_3Si), -1.7 (Me_2Si), -2.3 (Me_2Si). ^{19}F NMR (δ ppm): -132.7 (dd, $^3J_{\text{F,F}} = 24$ Hz, $^4J_{\text{F,F}} = 7$ Hz, *o*-ArF), -158.1 (t, $^3J_{\text{F,F}} = 21$ Hz, *p*-ArF), -164.3 (dt, $^3J_{\text{F,F}} = 24$ Hz, $^4J_{\text{F,F}} = 8$ Hz, *m*-ArF). ^{29}Si NMR (δ ppm): -6.0 (Me_3Si), -8.6 (Me_3Si), -22.6 (Me_2Si), -115.3 (d, $^3J_{\text{Si,P}} = 4$ Hz, Si_q). ^{31}P NMR (δ ppm): -7.6.

Triethylphosphino[2-cyano-2-stanna-1,1,3,3-tetrakis(trimethylsilyl)tetramethylcyclopentasilan-2-yl]gold(I)-(12). A mixture of AuCN (65 mg, 0.29 mmol) and 11 (204 mg, 0.29 mmol) was suspended in toluene (8 mL) and stirred for 2 h at rt. During the stirring the suspension turned into a clear brown solution. Half of the solvent was removed under reduced pressure and stored for 36 h at -60 °C. Colorless crystals of 12 (266 mg, 97%) could be isolated by decantation. ^1H NMR (δ in ppm): 0.84 (dq, $^3J_{\text{HH}} = 7.7$ Hz, $^2J_{\text{PH}} = 8.1$ Hz, 6H, $\text{P}(\text{CH}_2\text{CH}_3)_3$), 0.53 (dt, $^3J_{\text{HH}} = 7.7$ Hz, $^3J_{\text{PH}} = 17.8$ Hz, 9H, $\text{P}(\text{CH}_2\text{CH}_3)_3$), 0.42 (s, 18H, SiMe_3), 0.33 (s, 6H, SiMe_2), 0.27 (s, 18H, SiMe_3), 0.22 (s, 6H, SiMe_2). ^{13}C NMR (δ in ppm): 17.8 (d, $^2J_{\text{PC}} = 25.2$ Hz, $\text{P}(\text{CH}_2\text{CH}_3)_3$), 8.2 ($\text{P}(\text{CH}_2\text{CH}_3)_3$), 3.2 (SiMe_3),

2.9 (SiMe_3), -1.3 (SiMe_2), -1.6 (SiMe_2), CN could not be detected. ^{29}Si NMR (δ in ppm): -4.4, -7.4, -19.1, -125.8. ^{31}P NMR (δ in ppm): 49.5 (br). ^{119}Sn NMR (δ in ppm): -126.0 (d, $^2J_{\text{PSn}} = 1633$ Hz). Anal. Calcd for $\text{C}_{23}\text{H}_{63}\text{AuNPSi}_8\text{Sn}$ (925.09): C 29.86, H 6.86, N 1.51. Found: C 29.33, H 6.72, N 1.84.

Triethylphosphino[2-cyano-2-stanna-1,1,3,3-tetrakis(trimethylsilyl)tetramethylcyclopentasilan-2-yl]gold(I)-B(C₆F₅)₃ (13). Reaction was done according to the procedure for 5 using tris(pentafluorophenyl)borane (51 mg, 0.10 mmol) and 12 (70 mg, 0.10 mmol). Colorless crystals of 13 (103 mg, 85%) were obtained. Mp: 155–157 °C (dec). ^1H NMR (δ ppm): 1.09 (m, 6H, PCH_2CH_3), 0.79 (m, 9H, CH_2CH_3), 0.36 (s, 18H, Me_3Si), 0.33 (s, 6H, Me_2Si), 0.26 (s, 6H, Me_2Si), 0.23 (s, 18H, Me_3Si). ^{11}B NMR (δ ppm): -11.2. ^{13}C NMR (δ ppm): 149.9 (dm, $^1J_{\text{F,C}} = 239$ Hz, CF), 140.8 (dm, $^1J_{\text{F,C}} = 249$ Hz, CF), 137.9 (dm, $^1J_{\text{F,C}} = 249$ Hz, CF), 118.3 (m, CB), 18.1 (d, $^1J_{\text{C,P}} = 27$ Hz, PCH_2CH_3), 8.6 (CH_2CH_3), 3.5 (Me_3Si), 2.7 (Me_3Si), -1.1 (Me_2Si), -1.6 (Me_2Si), CN could not be detected. ^{19}F NMR (δ ppm): -132.6 (dd, $^3J_{\text{F,F}} = 24$ Hz, $^4J_{\text{F,F}} = 8$ Hz, *o*-ArF), -158.1 (t, $^3J_{\text{F,F}} = 21$ Hz, *p*-ArF), -164.4 (dt, $^3J_{\text{F,F}} = 24$ Hz, $^4J_{\text{F,F}} = 6$ Hz, *m*-ArF). ^{29}Si NMR (δ ppm): -3.9 (Me_3Si), -7.1 (Me_3Si), -20.0 (d, $^4J_{\text{Si,P}} = 4$ Hz, Me_2Si), -122.7 (d, $^3J_{\text{Si,P}} = 9$ Hz, Si_q). ^{31}P NMR (δ ppm): 50.1 ($^2J_{\text{P,119Sn}} = 1536$ Hz, $^2J_{\text{P,117Sn}} = 1467$ Hz). ^{119}Sn NMR (δ ppm): 31.1 (d, $^2J_{\text{Sn,P}} = 1545$ Hz).

■ ASSOCIATED CONTENT

Supporting Information

ORTEP plots of complexes 4, 6, 7, 10, and 13 as well as crystallographic information for complexes 3–8, 10, 12, and 13 in CIF format. In addition ^1H , ^{13}C , ^{29}Si , ^{19}F , and ^{119}Sn NMR spectra of borane adducts 5, 6, 9, 10, and 13, for which no elemental analyses were obtained, are provided as a measure of purity. This material is available free of charge via the Internet at <http://pubs.acs.org>.

■ AUTHOR INFORMATION

Corresponding Authors

*E-mail: christoph.marschner@tugraz.at.

*E-mail: baumgartner@tugraz.at.

Author Contributions

The manuscript was written through contributions of all authors. All authors have given approval to the final version of the manuscript.

Notes

The authors declare no competing financial interest.

■ ACKNOWLEDGMENTS

Support for this study was provided by the Austrian Science Fund (FWF) via the projects P-22678 (C.M.) and P-25124 (J.B.). Help provided by Prof. Karl Gatterer in attempts to obtain solution emission spectra of complexes 3 and 5 is gratefully acknowledged. Dedicated to Prof. Gerhard Roewer (Bergakademie Freiberg) on the occasion of his 75th birthday in recognition of his numerous accomplishments in organo-silicon chemistry

■ REFERENCES

- Beletskaya, I. P.; Cheprakov, A. V. *Coord. Chem. Rev.* **2004**, *248*, 2337–2364.
- Siemens, P.; Livingston, R. C.; Diederich, F. *Angew. Chem., Int. Ed.* **2000**, *39*, 2632–2657.
- Brand, J. P.; Waser, J. *Chem. Soc. Rev.* **2012**, *41*, 4165–4179.
- Hashmi, A. S. K. In *Silver in Organic Chemistry*; Harmata, M., Ed.; John Wiley & Sons: Hoboken, NJ, 2010.
- Krause, N.; Aksin-Artok, Ö.; Asikainen, M.; Breker, V.; Deutsch, C.; Erdsack, J.; Fan, H.-T.; Gockel, B.; Minkler, S.; Poonoth, M.;

- Sawama, Y.; Sawama, Y.; Sun, T.; Volz, F.; Winter, C. *J. Organomet. Chem.* **2012**, *704*, 1–8.
- (6) Glockling, F.; Hooton, K. A. *J. Chem. Soc.* **1962**, 2658–2661.
- (7) Dilts, J. A.; Johnson, M. P. *Inorg. Chem.* **1966**, *5*, 2079–2081.
- (8) Dias, H. V. R.; Ayers, A. E. *Polyhedron* **2002**, *21*, 611–618.
- (9) Anandhi, U.; Sharp, P. R. *Inorg. Chim. Acta* **2006**, *359*, 3521–3526.
- (10) Cabeza, J. A.; Fernández-Colinas, J. M.; García-Álvarez, P.; Polo, D. *Inorg. Chem.* **2012**, *51*, 3896–3903.
- (11) Klett, J.; Klinkhammer, K. W.; Niemeyer, M. *Chem.—Eur. J.* **1999**, *5*, 2531–2536.
- (12) York, J. T.; Young, V. G.; Tolman, W. B. *Inorg. Chem.* **2006**, *45*, 4191–4198.
- (13) Boehme, C.; Frenking, G. *Organometallics* **1998**, *17*, 5801–5809.
- (14) Attempts to measure solution emission spectra of **3** and **5** in toluene were undertaken with different emission wavelengths employing the conditions outlined for the germylene complexes mentioned in ref 9. No fluorescence was observed in any case.
- (15) Arp, H.; Marschner, C.; Baumgartner, J.; Zark, P.; Müller, T. *J. Am. Chem. Soc.* **2013**, *135*, 7949–7959.
- (16) Hlina, J. Ph.D. thesis, Technische Universität Graz: Graz, 2013.
- (17) Walewska, M. Ph.D. thesis, Technische Universität Graz, ongoing.
- (18) Arp, H.; Baumgartner, J.; Marschner, C.; Müller, T. *J. Am. Chem. Soc.* **2011**, *133*, 5632–5635.
- (19) Hlina, J.; Baumgartner, J.; Marschner, C.; Albers, L.; Müller, T. *Organometallics* **2013**, *32*, 3404–3410.
- (20) Arp, H.; Baumgartner, J.; Marschner, C.; Zark, P.; Müller, T. *J. Am. Chem. Soc.* **2012**, *134*, 10864–10875.
- (21) Hlina, J.; Baumgartner, J.; Marschner, C.; Zark, P.; Müller, T. *Organometallics* **2013**, *32*, 3300–3308.
- (22) Bergquist, C.; Bridgewater, B. M.; Harlan, C. J.; Norton, J. R.; Friesner, R. A.; Parkin, G. *J. Am. Chem. Soc.* **2000**, *122*, 10581–10590.
- (23) Isab, A. A.; Hussain, M. S.; Akhtar, M. N.; Wazeer, M. I. M.; Al-Arfaj, A. R. *Polyhedron* **1999**, *18*, 1401–1409.
- (24) Zangger, K.; Armitage, I. M. *Met. Based Drugs* **1999**, *6*, 239–245.
- (25) Socol, S. M.; Verkade, J. G. *Inorg. Chem.* **1984**, *23*, 3487–3493.
- (26) Price, S. J. B.; Brevard, C.; Pagelot, A.; Sadler, P. J. *Inorg. Chem.* **1985**, *24*, 4278–4281.
- (27) Baker, L. J.; Bowmaker, G. A.; Camp, D.; Effendy; Healy, P. C.; Schmidbaur, H.; Steigelmann, O.; White, A. H. *Inorg. Chem.* **1992**, *31*, 3656–3662.
- (28) Sanghani, D. V.; Smith, P. J.; Allen, D. W.; Taylor, B. F. *Inorg. Chim. Acta* **1982**, *59*, 203–206.
- (29) Findeis, B.; Gade, L. H.; Scowen, I. J.; McPartlin, M. *Inorg. Chem.* **1997**, *36*, 960–961.
- (30) Wagner, H.; Schubert, U. *Chem. Ber.* **1990**, *123*, 2101–2107.
- (31) Conquest Version 1.16 was used.
- (32) Tripathi, U. M.; Wegner, G. L.; Schier, A.; Jockisch, A.; Schmidbaur, H. *Z. Naturforsch. B* **1998**, *53*, 939–945.
- (33) Bauer, A.; Schneider, W.; Schmidbaur, H. *Inorg. Chem.* **1997**, *36*, 2225–2226.
- (34) Leung, W.-P.; So, C.-W.; Kan, K.-W.; Chan, H.-S.; Mak, T. C. W. *Organometallics* **2005**, *24*, 5033–5037.
- (35) Bauer, A.; Schmidbaur, H. *J. Am. Chem. Soc.* **1996**, *118*, 5324–5325.
- (36) Contel, M.; Hellmann, K. W.; Gade, L. H.; Scowen, I. J.; McPartlin, M.; Laguna, M. *Inorg. Chem.* **1996**, *35*, 3713–3715.
- (37) Matioszek, D.; Kocsor, T. G.; Castel, A.; Nemes, G. N.; Escudie, J.; Saffon, N. *Chem. Commun.* **2012**, *48*, 3629–3631.
- (38) Zhao, N.; Zhang, J.; Yang, Y.; Chen, G.; Zhu, H.; Roesky, H. W. *Organometallics* **2013**, *32*, 762–769.
- (39) Weinert, C. S.; Fanwick, P. E.; Rothwell, I. P. *Acta Crystallogr., Sect. E* **2002**, *58*, m718–m720.
- (40) Ayers, A. E.; Dias, H. V. R. *Inorg. Chem.* **2002**, *41*, 3259–3268.
- (41) Dias, H. V. R.; Wang, Z. *Inorg. Chem.* **2000**, *39*, 3890–3893.
- (42) Zhao, N.; Zhang, J.; Yang, Y.; Zhu, H.; Li, Y.; Fu, G. *Inorg. Chem.* **2012**, *51*, 8710–8718.
- (43) West, J. K.; Fondong, G. L.; Noll, B. C.; Stahl, L. *Dalton Trans.* **2013**, *42*, 3835–3842.
- (44) Leung, W.-P.; So, C.-W.; Chong, K.-H.; Kan, K.-W.; Chan, H.-S.; Mak, T. C. W. *Organometallics* **2006**, *25*, 2851–2858.
- (45) Orlov, N. A.; Bochkarev, L. N.; Nikitinsky, A. V.; Kropotova, V. Y.; Zakharov, L. N.; Fukin, G. K.; Khorshev, S. Y. *J. Organomet. Chem.* **1998**, *560*, 21–25.
- (46) Arii, H.; Nakadate, F.; Mochida, K. *Organometallics* **2009**, *28*, 4909–4911.
- (47) Orlov, N. A.; Bochkarev, L. N.; Nikitinsky, A. V.; Zhiltsov, S. F.; Zakharov, L. N.; Fukin, G. K.; Khorshev, S. Y. *J. Organomet. Chem.* **1997**, *547*, 65–69.
- (48) Findeis, B.; Contel, M.; Gade, L. H.; Laguna, M.; Gimeno, M. C.; Scowen, I. J.; McPartlin, M. *Inorg. Chem.* **1997**, *36*, 2386–2390.
- (49) Fischer, J.; Gaderbauer, W.; Baumgartner, J.; Marschner, C. *Heterocycles* **2006**, *67*, 507–510.
- (50) Fischer, R.; Frank, D.; Gaderbauer, W.; Kayser, C.; Mechtler, C.; Baumgartner, J.; Marschner, C. *Organometallics* **2003**, *22*, 3723–3731.
- (51) Brown, Z. D.; Vasko, P.; Fettingner, J. C.; Tuononen, H. M.; Power, P. P. *J. Am. Chem. Soc.* **2012**, *134*, 4045–4048.
- (52) Hihara, G.; Hynes, R. C.; Lebus, A.-M.; Rivière-Baudet, M.; Wharf, I.; Onyszczuk, M. *J. Organomet. Chem.* **2000**, *598*, 276–285.
- (53) Schlemper, E. O.; Britton, D. *Inorg. Chem.* **1966**, *5*, 511–514.
- (54) Konnert, J. H.; Britton, D.; Chow, Y. M. *Acta Crystallogr. B* **1972**, *28*, 180–187.
- (55) Avalle, P.; Harris, R. K.; Hanika-Heidl, H.; Dieter Fischer, R. *Solid State Sci.* **2004**, *6*, 1069–1076.
- (56) Pangborn, A. B.; Giardello, M. A.; Grubbs, R. H.; Rosen, R. K.; Timmers, F. J. *Organometallics* **1996**, *15*, 1518–1520.
- (57) Morris, G. A.; Freeman, R. *J. Am. Chem. Soc.* **1979**, *101*, 760–762.
- (58) Helmer, B. J.; West, R. *Organometallics* **1982**, *1*, 877–879.
- (59) Morris, K. F.; Johnson, C. S. *J. Am. Chem. Soc.* **1993**, *115*, 4291–4299.
- (60) Glanzer, S.; Zangger, K. *Chem.—Eur. J.* **2014**, *20*, 11171–11175.
- (61) SAINTPLUS: Software Reference Manual, Version 6.45; Bruker-AXS: Madison, WI, 1997–2003.
- (62) Sheldrick, G. M. SADABS, Version 2.10; Bruker AXS Inc.: Madison, WI, 2003.
- (63) Sheldrick, G. M. *Acta Crystallogr. A* **2007**, *64*, 112–122.